

# IMEX Runge-Kutta schemes for reaction-diffusion equations

Toshiyuki Koto

*Graduate School of Information Science  
Nagoya University  
Nagoya 464-8601, Japan  
email: koto@is.nagoya-u.ac.jp*

---

## Abstract

A fundamental research is carried out into convergence and stability properties of IMEX (implicit-explicit) Runge-Kutta schemes applied to reaction-diffusion equations. It is shown that a fully discrete scheme converges if it satisfies certain conditions using a technique of the  $B$ -convergence analysis, developed by Burrage, Hundsdorfer & Verwer in 1986. Stability of the schemes is also examined on the basis of a scalar test equation, proposed by Frank, Hundsdorfer & Verwer in 1997.

*Key words:* IMEX schemes, reaction-diffusion equations, stability analysis

---

## 1 Introduction

We consider initial-boundary value problems of the form

$$\begin{aligned}\frac{\partial \mathbf{u}}{\partial t} &= L\mathbf{u} + g(t, x, \mathbf{u}), \quad 0 \leq t \leq T, \quad x \in \Omega, \\ \Phi_b \mathbf{u}(t, x) &= \varphi(t, x), \quad 0 \leq t \leq T, \quad x \in \partial\Omega, \\ \mathbf{u}(0, x) &= \mathbf{u}_0(x), \quad x \in \Omega.\end{aligned}\tag{1.1}$$

Here,  $\mathbf{u} = \mathbf{u}(t, x)$  is an  $\mathbb{R}^m$ -valued unknown function,  $\Omega$  is a bounded domain in  $\mathbb{R}$ ,  $\mathbb{R}^2$ , or  $\mathbb{R}^3$  with the boundary  $\partial\Omega$ ,  $L$  is a linear partial differential operator with respect to  $x$ , and  $g$  is a function from  $[0, T] \times \Omega \times \mathbb{R}^m$  to  $\mathbb{R}^m$ . Also,  $\Phi_b$  is a boundary operator, and  $\varphi(t, x)$ ,  $\mathbf{u}_0(x)$  are given functions. Many important reaction-diffusion equations (see, e.g., [11]) are represented in this form with

$$L = \text{diag}(D_1\Delta, D_2\Delta, \dots, D_m\Delta),\tag{1.2}$$

where  $\Delta$  is the Laplace operator and  $D_i$  are nonnegative constants.

A well-known approach in the numerical solution of evolutionary problems in partial differential equations (PDEs) is the method of lines (MOL). In this approach a PDE is first discretized in space by finite difference or finite element techniques to be converted into a system of ordinary differential equations (ODEs). Let  $\Omega_h \subset \overline{\Omega}$  be a grid with mesh width  $h > 0$ , and let  $\mathbf{V}_h$  denote the vector space of all functions from  $\Omega_h$  to  $\mathbb{R}^m$ . An MOL approximation of (1.1) is written in the form

$$\frac{du}{dt} = L_h u + \varphi_h(t) + g_h(t, u). \quad (1.3)$$

Here,  $u = u_h$  is an approximate function of  $\mathbf{u}$  such that  $u(t) \in \mathbf{V}_h$  for  $t \in [0, T]$ ,  $L_h$  is a difference approximation of  $L$ ,  $g_h$  is a function from  $[0, T] \times \mathbf{V}_h$  to  $\mathbf{V}_h$ , defined by  $g_h(t, v)(x) = g(t, x, v(x))$ ,  $x \in \Omega_h$ , for  $t \in [0, T]$  and  $v \in \mathbf{V}_h$ , and  $\varphi_h(t)$  is a function determined from the boundary condition.

Ordinarily,  $L_h u$  on the right hand side of (1.3) gives a stiff term. If the  $g_h$ -term is non-stiff or mildly stiff, an IMEX (implicit-explicit) Runge-Kutta scheme (see, e.g., [7], Chapt. IV, Sect. 4) is a proper choice for solving the equation (1.3). Let us consider a pair of two Runge-Kutta methods defined by the arrays

$$\begin{array}{c|cccccc} 0 & 0 & 0 & \cdots & 0 & 0 \\ c_2 & a_{21} & a_{22} & 0 & \cdots & 0 \\ c_3 & a_{31} & a_{32} & a_{33} & & \vdots \\ \vdots & \vdots & & \ddots & 0 & \\ c_s & a_{s1} & a_{s2} & \cdots & a_{s,s-1} & a_{ss} \\ \hline & b_1 & b_2 & \cdots & b_{s-1} & b_s \end{array}, \quad \begin{array}{c|cccccc} 0 & 0 & 0 & \cdots & 0 & 0 \\ c_2 & \hat{a}_{21} & 0 & \cdots & 0 & \\ c_3 & \hat{a}_{31} & \hat{a}_{32} & 0 & & \vdots \\ \vdots & \vdots & & \ddots & 0 & \\ c_s & \hat{a}_{s1} & \hat{a}_{s2} & \cdots & \hat{a}_{s,s-1} & 0 \\ \hline & \hat{b}_1 & \hat{b}_2 & \cdots & \hat{b}_{s-1} & \hat{b}_s \end{array}, \quad (1.4)$$

with the same abscissae

$$c_i = \sum_{j=1}^i a_{ij} = \sum_{j=1}^{i-1} \hat{a}_{ij}, \quad i = 1, \dots, s. \quad (1.5)$$

For simplicity, we assume that  $0 \leq c_i \leq 1$ . The left formula determines a diagonally implicit (semi-implicit) Runge-Kutta method, the right formula an explicit Runge-Kutta method. In addition, let  $\Delta t > 0$  be a step size and define the step point  $t_n = n\Delta t$  for integer  $n$ . By applying the left formula to the linear part of (1.3) and the right formula to the nonlinear part, we obtain

the following scheme for the problem (1.1):

$$\begin{aligned}
U_{n,i} &= u_n + \Delta t \sum_{j=1}^i a_{ij} (L_h U_{n,j} + \varphi_h(t_{n,j})) + \Delta t \sum_{j=1}^{i-1} \hat{a}_{ij} g_h(t_{n,j}, U_{n,j}), \\
i &= 1, \dots, s, \\
u_{n+1} &= u_n + \Delta t \sum_{i=1}^s b_i (L_h U_{n,i} + \varphi_h(t_{n,i})) + \Delta t \sum_{i=1}^s \hat{b}_i g_h(t_{n,i}, U_{n,i}).
\end{aligned} \tag{1.6}$$

Here,  $u_n$  is an approximate value of  $u(t_n)$ ,  $t_{n,i} := t_n + c_i \Delta t$ , and  $U_{n,i}$  are intermediate variables, which are successively computed by solving linear equations. The initial value  $u_0$  is given by  $u_0(x) = \mathbf{u}_0(x)$ ,  $x \in \Omega_h$ .

The IMEX Euler scheme (see, e.g., [6]) is the simplest example, which is a combination of the implicit and explicit Euler methods

$$\begin{array}{c|cc} 0 & 0 & 0 \\ \hline 1 & 0 & 1 \\ \hline & 0 & 1 \end{array} , \quad \begin{array}{c|cc} 0 & 0 & 0 \\ \hline 1 & 1 & 0 \\ \hline & 1 & 0 \end{array} . \tag{1.7}$$

In this case, the scheme (1.6) is reduced to

$$u_{n+1} = u_n + \Delta t (L_h u_{n+1} + \varphi_h(t_{n+1})) + \Delta t g_h(t_n, u_n). \tag{1.8}$$

Several authors [1,3,8,13] have already studied properties of IMEX Runge-Kutta schemes for PDEs. But, they mainly consider advection-diffusion equations or more general PDEs. Fundamental properties for reaction-diffusion equations, which seem easier to treat, are not clarified. In this paper, we study convergence and stability properties of IMEX Runge-Kutta schemes focusing on their application to reaction-diffusion problems.

The paper is organized as follows. In the next section (Sect. 2) we prove a theorem which guarantees convergence of fully discrete IMEX Runge-Kutta schemes using a technique of the  $B$ -convergence analysis. The result is confirmed by a numerical experiment in Sect. 3. Another numerical experiment concerned with stability of the schemes is also presented in the same section; in particular, an instability phenomenon for an IMEX scheme is presented. The phenomenon is analyzed in Sect. 4. We examine stability of IMEX Runge-Kutta schemes using a scalar test equation, and show that some IMEX schemes possess a good stability property for reaction-diffusion equations.

## 2 Convergence of fully discrete schemes

We assume the following conditions for the problem (1.1) and the MOL approximation (1.3):

The exact solution  $\mathbf{u}(t, x)$  is of class  $C^3$  with respect to  $t$ ;  $g(t, x, \mathbf{u})$  is of class  $C^2$  with respect to  $t, \mathbf{u}$  and (each component of) the derivative  $\partial g / \partial \mathbf{u}$  is bounded for  $(t, x, \mathbf{u}) \in [0, T] \times \Omega \times \mathbb{R}^m$ . Let  $\langle \cdot, \cdot \rangle = \langle \cdot, \cdot \rangle_h$  denote an inner product on  $\mathbf{V}_h$  and let  $\| \cdot \| = \| \cdot \|_h$  be the corresponding norm. We assume that  $L_h$  is dissipative with respect to  $\langle \cdot, \cdot \rangle$ , i.e.,

$$\langle L_h v, v \rangle \leq 0 \quad \text{for any } v \in \mathbf{V}_h. \quad (2.1)$$

In the case  $L_h$  is symmetric with respect to  $\langle \cdot, \cdot \rangle$ , i.e.,  $\langle L_h v, w \rangle = \langle v, L_h w \rangle$  for  $v, w \in \mathbf{V}_h$ , the condition (2.1) means that  $L_h$  is negative semidefinite; many difference approximations of the Laplace operator have this property.

As for the IMEX method (1.4), we consider the usual order conditions

$$\sum_{i=1}^s b_i = 1, \quad \sum_{i=1}^s \hat{b}_i = 1, \quad (2.2)$$

$$\sum_{i=1}^s b_i c_i = 1/2, \quad \sum_{i=1}^s \hat{b}_i c_i = 1/2, \quad (2.3)$$

and the following extra conditions. We use the standard symbols  $\mathbb{1} = [1, \dots, 1]^T$  and  $\mathbb{C}^- = \{z \in \mathbb{C} : \text{Re } z < 0\}$ .

(A) The diagonally implicit Runge-Kutta method is *A*-stable, *ASI*-stable, and *AS*-stable, i.e., the stability function  $r(z) = 1 + z b^T (I_s - zA)^{-1} \mathbb{1}$  satisfies

$$|r(z)| \leq 1 \quad \text{for any } z \in \mathbb{C}^-,$$

and all the components of  $(I_s - zA)^{-1}$  and  $z b^T (I_s - zA)^{-1}$  are bounded on  $\mathbb{C}^-$ .

(B) The rational functions

$$\phi(z) = \frac{b^T (I_s - zA)^{-1} \boldsymbol{\xi}}{b^T (I_s - zA)^{-1} \mathbb{1}}, \quad \hat{\phi}(z) = \frac{b^T (I_s - zA)^{-1} \hat{\boldsymbol{\xi}}}{b^T (I_s - zA)^{-1} \mathbb{1}} \quad (2.4)$$

are bounded on  $\mathbb{C}^-$ , where

$$\begin{aligned} \boldsymbol{\xi} &= [0, \xi_2, \dots, \xi_s]^T, \quad \hat{\boldsymbol{\xi}} = [0, \hat{\xi}_2, \dots, \hat{\xi}_s]^T, \\ \xi_i &= c_i^2/2 - \sum_{j=1}^i a_{ij} c_j, \quad \hat{\xi}_i = \sum_{j=1}^i a_{ij} c_j - \sum_{j=1}^{i-1} \hat{a}_{ij} c_j. \end{aligned}$$

We also define the spatial truncation error  $\alpha_h(t)$  by

$$\alpha_h(t) = \mathbf{u}'_h(t) - L_h \mathbf{u}_h(t) - \varphi_h(t) - g_h(t, \mathbf{u}_h(t)), \quad (2.5)$$

where  $\mathbf{u}_h(t)$  is a  $\mathbf{V}_h$ -valued function obtained by restricting the variable  $x$  of the exact solution  $\mathbf{u}$  onto  $\Omega_h$ . For simplicity, we consider step sizes of the form  $\Delta t = T/N$  with positive integer  $N$ . Then, we have the following theorem.

**Theorem 2.1** *If the coefficients (1.4) satisfy (2.2) and (A), then there are positive constants  $\tau_1, C_1$  such that*

$$\max_{1 \leq n \leq N} \|u_n - \mathbf{u}_h(t_n)\| \leq C_1 \left( \Delta t + \max_{0 \leq t \leq T} \|\alpha_h(t)\| \right) \quad (2.6)$$

*holds for any  $\Delta t \leq \tau_1$ . If, in addition, (1.4) satisfy (2.3) and (B), then there are positive constants  $\tau_2, C_2$  such that*

$$\max_{1 \leq n \leq N} \|u_n - \mathbf{u}_h(t_n)\| \leq C_2 \left( \Delta t^2 + \max_{0 \leq t \leq T} \|\alpha_h(t)\| \right) \quad (2.7)$$

*holds for any  $\Delta t \leq \tau_2$ .*

The second order convergence is, in a sense, optimal. It is known that Runge-Kutta approximations for PDEs suffer from order reduction phenomena. The order of time-stepping in the fully discrete scheme is, in general, less than that of the underlying Runge-Kutta scheme. In particular, the order of a diagonally implicit Runge-Kutta scheme for PDEs does not exceed two [15] (see also [9,14] on order reduction phenomena of Runge-Kutta schemes in the PDE context). This property is inherited by IMEX Runge-Kutta schemes.

The proof of the theorem is carried out by the same argument as in the proof of Theorem 3.3 of Burrage, Hundsdorfer & Verwer [2]. The following lemma (see, e.g., [5], IV.11) is the basis of the proof.

**Lemma 2.2 (Theorem of von Neumann)** *Let  $\psi(z)$  be a rational function which has no pole in  $\mathbb{C}^-$ . Then, under the condition (2.1), we have*

$$\|\psi(\Delta t L_h)\| \leq \sup_{\operatorname{Re} z \leq 0} |\psi(z)|. \quad (2.8)$$

*Proof of Theorem 2.1.* Replacing  $U_{n,i}, u_n$  and  $u_{n+1}$  in the scheme (1.6) with  $\mathbf{u}_h(t_{n,i}), \mathbf{u}_h(t_n)$  and  $\mathbf{u}_h(t_{n+1})$ , respectively, we obtain the recurrence relation

$$\mathbf{u}_h(t_{n,i}) = \mathbf{u}_h(t_n) + \Delta t \sum_{j=1}^i a_{ij} \left( L_h \mathbf{u}_h(t_{n,j}) + \varphi_h(t_{n,j}) \right)$$

$$+ \Delta t \sum_{j=1}^{i-1} \hat{a}_{ij} g_h(t_{n,j}, \mathbf{u}_h(t_{n,j})) + r_{n,i}, \quad (2.9)$$

$$\begin{aligned} \mathbf{u}_h(t_{n+1}) &= \mathbf{u}_h(t_n) + \Delta t \sum_{i=1}^s b_i \left( L_h \mathbf{u}_h(t_{n,i}) + \varphi_h(t_{n,i}) \right) \\ &\quad + \Delta t \sum_{i=1}^s \hat{b}_i g_h(t_{n,i}, \mathbf{u}_h(t_{n,i})) + \rho_n \end{aligned} \quad (2.10)$$

with the residuals  $r_{n,i}$  and  $\rho_n$ . By (2.5) and (1.5),  $r_{n,i}$  is expanded as

$$\begin{aligned} r_{n,i} &= \mathbf{u}_h(t_{n,i}) - \mathbf{u}_h(t_n) - \Delta t \sum_{j=1}^i a_{ij} \left[ \mathbf{u}'_h(t_{n,j}) - g_h(t_{n,j}, \mathbf{u}_h(t_{n,j})) - \alpha_h(t_{n,j}) \right] \\ &\quad - \Delta t \sum_{j=1}^{i-1} \hat{a}_{ij} g_h(t_{n,j}, \mathbf{u}_h(t_{n,j})) \\ &= \Delta t^2 \xi_i \mathbf{u}''_h(t_n) + \Delta t^2 \hat{\xi}_i \mathbf{g}_h^{(1)}(t_n) + \Delta t \sum_{j=1}^i a_{ij} \alpha_h(t_{n,j}) + O(\Delta t^3). \end{aligned} \quad (2.11)$$

Here,  $\mathbf{g}_h^{(1)}(t_n)$  is an element of  $\mathbf{V}_h$  whose value for  $x \in \Omega_h$  is given by

$$\mathbf{g}_h^{(1)}(t_n) = \frac{\partial g}{\partial t}(t_n, x, \mathbf{u}(t_n, x)) + \frac{\partial g}{\partial \mathbf{u}}(t_n, x, \mathbf{u}(t_n, x)) \frac{\partial \mathbf{u}}{\partial t}(t_n, x),$$

and  $O(\Delta t^3)$  denotes a term whose component for each  $x \in \Omega_h$  is of  $O(\Delta t^3)$ .

Subtracting (1.6) from (2.9) and (2.10), we have the recurrence relation

$$\begin{cases} \delta_{n,i} = \varepsilon_n + \Delta t \sum_{j=1}^i a_{ij} L_h \delta_{n,j} + \Delta t \sum_{j=1}^{i-1} \hat{a}_{ij} J_{n,j} \delta_{n,j} + r_{n,i}, \\ \varepsilon_{n+1} = \varepsilon_n + \Delta t \sum_{i=1}^s b_i L_h \delta_{n,i} + \Delta t \sum_{i=1}^s \hat{b}_i J_{n,i} \delta_{n,i} + \rho_n, \end{cases} \quad (2.12)$$

for the errors

$$\delta_{n,i} = \mathbf{u}_h(t_{n,i}) - U_{n,i}, \quad \varepsilon_n = \mathbf{u}_h(t_n) - u_n,$$

where  $J_{n,i}$  is a function from  $\Omega_h$  to  $\mathbb{R}^{m \times m}$  whose value for  $x \in \Omega_h$  is

$$J_{n,i}(x) = \int_0^1 \frac{\partial g}{\partial \mathbf{u}}(t_{n,i}, x, (1-\theta)U_{n,i}(x) + \theta \mathbf{u}(t_{n,i}, x)) d\theta,$$

and the multiplication  $J_{n,i} \delta_{n,i}$  is component-wise for  $x \in \Omega_h$ . Putting

$$\mathbf{A} = A \otimes I, \widehat{\mathbf{A}} = \widehat{A} \otimes I, \mathbf{b} = b \otimes I, \widehat{\mathbf{b}} = \widehat{b} \otimes I, \mathbf{I} = I_s \otimes I, \\ Z = \Delta t (I_s \otimes L_h), W_n = \Delta t \operatorname{diag}(J_{n,1}, \dots, J_{n,s}),$$

$$\delta_n = \begin{bmatrix} \delta_{n,1} \\ \vdots \\ \delta_{n,s} \end{bmatrix}, r_n = \begin{bmatrix} r_{n,1} \\ \vdots \\ r_{n,s} \end{bmatrix},$$

where  $I$  is the identity map on  $\mathbf{V}_h$ , we can rewrite (2.12) in the form

$$\begin{cases} (\mathbf{I} - \mathbf{A}Z - \widehat{\mathbf{A}}W_n)\delta_n = \mathbb{1} \otimes \varepsilon_n + r^n, \\ \varepsilon_{n+1} = \varepsilon_n + (\mathbf{b}^T Z + \widehat{\mathbf{b}}^T W_n)\delta_n + \rho_n. \end{cases} \quad (2.13)$$

We now assume (2.2) and (A). From (2.2) and (2.5) it follows that

$$\rho_n = \Delta t \sum_{i=1}^s b_i \alpha_h(t_{n,i}) + O(\Delta t^2). \quad (2.14)$$

By the assumption that  $\partial g / \partial \mathbf{u}$  is bounded, there is a constant  $\gamma_0$  such that

$$\| J_{n,i} v \| \leq \gamma_0 \| v \| \quad \text{for any } v \in \mathbf{V}_h. \quad (2.15)$$

Thus, by the same argument as in the proof of Lemma 3.5 in [2], we can show that  $\mathbf{I} - \mathbf{A}Z - \widehat{\mathbf{A}}W_n$  is invertible if  $\Delta t$  is sufficiently small. Eliminating  $\delta_n$  from (2.13) we get

$$\varepsilon_{n+1} = \mathbf{R}_n \varepsilon_n + \mathbf{M}_n r_n + \rho_n, \quad (2.16)$$

where

$$\mathbf{R}_n = I + (\mathbf{b}^T Z + \widehat{\mathbf{b}}^T W_n)(\mathbf{I} - \mathbf{A}Z - \widehat{\mathbf{A}}W_n)^{-1}(\mathbb{1} \otimes I), \\ \mathbf{M}_n = (\mathbf{b}^T Z + \widehat{\mathbf{b}}^T W_n)(\mathbf{I} - \mathbf{A}Z - \widehat{\mathbf{A}}W_n)^{-1}.$$

By the same argument as in the proof of Lemma 3.6 in [2], we can also show that there are positive constants  $\gamma_1, \gamma_2, \tau_3$  such that

$$\| \mathbf{R}_n \| \leq 1 + \gamma_1 \Delta t, \quad \| \mathbf{M}_n r_n \| \leq \gamma_2 \sum_{i=1}^s \| r_{n,i} \| \quad (2.17)$$

for  $\Delta t \leq \tau_3$ . Hence, it follows from (2.14) and (2.16) that

$$\| \varepsilon_{n+1} \| \leq (1 + \gamma_1 \Delta t) \| \varepsilon_n \| + C_3 \left( \Delta t^2 + \Delta t \max_{0 \leq t \leq T} \| \alpha_h(t) \| \right) \quad (2.18)$$

for some constant  $C_3$  and sufficiently small  $\Delta t$ . This implies that

$$\|\varepsilon_n\| \leq e^{\gamma_1 T} \|\varepsilon_0\| + \frac{C_3(e^{\gamma_1 T} - 1)}{\gamma_1} \left( \Delta t + \max_{0 \leq t \leq T} \|\alpha_h(t)\| \right) \quad (2.19)$$

for  $1 \leq n \leq N$ . Letting  $C_1 = C_3(e^{\gamma_1 T} - 1)/\gamma_1$ , we have (2.6) since  $\|\varepsilon_0\| = 0$ .

Furthermore, we assume (2.3) and (B), and put

$$\begin{aligned} \eta_n &= \phi(\Delta t L_h) \mathbf{u}_h''(t_n) + \hat{\phi}(\Delta t L_h) \mathbf{g}_h^{(1)}(t_n), \\ w_n &= \boldsymbol{\xi} \otimes \mathbf{u}_h''(t_n) + \hat{\boldsymbol{\xi}} \otimes \mathbf{g}_h^{(1)}(t_n) - \mathbb{1} \otimes \eta_n. \end{aligned}$$

By the condition (B) and Lemma 2.2,  $\|\eta_n\|$  and  $\|w_n\|$  are bounded. Noticing that  $\mathbf{R}_n \eta_n = \eta_n + \mathbf{M}_n(\mathbb{1} \otimes \eta_n)$ , we can rewrite (2.16) as

$$\hat{\varepsilon}_{n+1} = \mathbf{R}_n \hat{\varepsilon}_n + \mathbf{M}_n \hat{r}_n + \hat{\rho}_n, \quad (2.20)$$

where

$$\begin{aligned} \hat{\varepsilon}_n &= \varepsilon_n + \Delta t^2 \eta_n, \quad \hat{r}_n = r_n - \Delta t^2 \boldsymbol{\xi} \otimes \mathbf{u}_h''(t_n) - \Delta t^2 \hat{\boldsymbol{\xi}} \otimes \mathbf{g}_h^{(1)}(t_n), \\ \hat{\rho}_n &= \rho_n + \Delta t^2 (\eta_{n+1} - \eta_n) + \Delta t^2 \mathbf{M}_n w_n. \end{aligned}$$

By (2.11),  $\hat{\rho}_n$  is represented as

$$\hat{r}_n = \begin{bmatrix} \hat{r}_{n,1} \\ \vdots \\ \hat{r}_{n,s} \end{bmatrix}, \quad \hat{r}_{n,i} = \Delta t \sum_{j=1}^i a_{ij} \alpha_h(t_{n,j}) + O(\Delta t^3). \quad (2.21)$$

Moreover, we have  $\mathbf{b}^T Z(\mathbf{I} - \mathbf{AZ})^{-1} w_n = 0$  by the definitions of  $\phi$  and  $\hat{\phi}$ . Hence, it follows from

$$\begin{aligned} (\mathbf{I} - \mathbf{AZ} - \widehat{\mathbf{A}}W_n)^{-1} &= (\mathbf{I} - \mathbf{AZ})^{-1} \\ &\quad + (\mathbf{I} - \mathbf{AZ})^{-1} \widehat{\mathbf{A}}W_n (\mathbf{I} - \mathbf{AZ} - \widehat{\mathbf{A}}W_n)^{-1} \end{aligned}$$

that

$$\begin{aligned} \mathbf{M}_n w_n &= \hat{\mathbf{b}}^T W_n (\mathbf{I} - \mathbf{AZ})^{-1} w_n \\ &\quad + (\mathbf{b}^T Z + \hat{\mathbf{b}}^T W_n) (\mathbf{I} - \mathbf{AZ})^{-1} \widehat{\mathbf{A}}W_n (\mathbf{I} - \mathbf{AZ} - \widehat{\mathbf{A}}W_n)^{-1} w_n. \end{aligned}$$



It is verified that this value is of  $O(\Delta t)$  by the *ASI*-stability and *AS*-stability of the implicit scheme, which, together with the usual order condition (2.3) and  $\eta_{n+1} - \eta_n = O(\Delta t)$ , implies that

$$\hat{\rho}_n = \Delta t \sum_{i=1}^s b_i \alpha_h(t_{n,i}) + O(\Delta t^3). \quad (2.22)$$

Hence, from (2.20) we have

$$\| \hat{\varepsilon}_{n+1} \| \leq (1 + \gamma_1 \Delta t) \| \hat{\varepsilon}_n \| + C_4 \left( \Delta t^3 + \Delta t \max_{0 \leq t \leq T} \| \alpha_h(t) \| \right) \quad (2.23)$$

for some constant  $C_4$ , which implies that

$$\| \hat{\varepsilon}_n \| \leq e^{\gamma_1 T} \Delta t^2 \| \eta_0 \| + \frac{C_4(e^{\gamma_1 T} - 1)}{\gamma_1} \left( \Delta t^2 + \max_{0 \leq t \leq T} \| \alpha_h(t) \| \right) \quad (2.24)$$

for  $1 \leq n \leq N$ . Using  $\| \varepsilon_n \| \leq \| \hat{\varepsilon}_n \| + \Delta t^2 \| \eta_n \|$  and rewriting the constants, we finally obtain (2.7).  $\square$

### 3 Numerical examples

We present some numerical results for problems in one-dimensional PDEs in the case  $\Omega = (0, 1)$ . To test the accuracy of IMEX Runge-Kutta schemes, we adopt a model problem of the form

$$\begin{aligned} \frac{\partial \mathbf{u}}{\partial t} &= \frac{\partial^2 \mathbf{u}}{\partial x^2} + g(t, x, \mathbf{u}), \quad 0 \leq t \leq 1, \quad x \in \Omega, \\ \mathbf{u}(t, 0) &= \beta_0(t), \quad \mathbf{u}(t, 1) = \beta_1(t), \quad 0 \leq t \leq 1, \\ \mathbf{u}(0, x) &= \mathbf{u}_0(x), \quad x \in \Omega, \end{aligned} \quad (3.1)$$

where

$$\begin{aligned} g(t, x, \mathbf{u}) &= \mathbf{u} - \mathbf{u}^2 + 3e^{t-x} \cos(t+x) + e^{2(t-x)} \sin^2(t+x), \\ \beta_0(t) &= e^t \sin t, \quad \beta_1(t) = e^{t-1} \sin(t+1), \quad \mathbf{u}_0(x) = e^{-x} \sin x. \end{aligned}$$

The exact solution is given by

$$\mathbf{u}(t, x) = e^{t-x} \sin(t+x).$$

Let  $M$  be a positive integer,  $h = 1/M$ , and let  $\Omega_h$  be a uniform grid with nodes  $x_j = jh$ ,  $j = 1, \dots, M-1$ . By replacing the second order spatial derivative with the second order centered difference, we obtain an MOL approximation

$$\frac{du}{dt} = L_h u + \varphi_h(t) + g_h(t, u), \quad (3.2)$$

where  $u(t) = [u^1(t), \dots, u^{M-1}(t)]^T$ ,  $u^j(t) \approx \mathbf{u}(t, x_j)$ , and

$$L_h = \frac{1}{h^2} \begin{bmatrix} -2 & 1 & 0 & \cdots & 0 \\ 1 & -2 & 1 & \cdots & 0 \\ 0 & 1 & -2 & \cdots & 0 \\ \vdots & \vdots & \vdots & \ddots & \vdots \\ 0 & 0 & \cdots & 1 & -2 \end{bmatrix}, \quad \varphi_h(t) = \frac{1}{h^2} \begin{bmatrix} \beta_0(t) \\ 0 \\ \vdots \\ 0 \\ \beta_1(t) \end{bmatrix}. \quad (3.3)$$

One of the simplest IMEX Runge-Kutta schemes which satisfy all the conditions of Theorem 2.1 is the IMEX trapezoidal scheme (see, e.g., [7], p.391)

$$\begin{array}{c|cc} 0 & 0 & 0 \\ \hline 1 & 1/2 & 1/2 \\ \hline & 1/2 & 1/2 \end{array}, \quad \begin{array}{c|cc} 0 & 0 & 0 \\ \hline 1 & 1 & 0 \\ \hline & 1/2 & 1/2 \end{array}. \quad (3.4)$$

The usual order conditions (2.2) and (2.3) are clearly satisfied. It follows from

$$r(z) = \frac{1+z/2}{1-z/2}, \quad (I_2 - zA)^{-1} = \begin{bmatrix} 1 & 0 \\ z/(2-z) & 2/(2-z) \end{bmatrix},$$

$$zb^T(I_2 - zA)^{-1} = [z/(2-z), z/(2-z)]$$

that the (implicit) trapezoidal scheme satisfies (A). In addition,  $\boldsymbol{\xi} = [0, 0]^T$  and  $\widehat{\boldsymbol{\xi}} = [0, 1/2]^T$ . Hence,

$$\phi(z) = \frac{b^T(I_2 - zA)^{-1}\boldsymbol{\xi}}{b^T(I_2 - zA)^{-1}\mathbb{1}} = 0, \quad \widehat{\phi}(z) = \frac{b^T(I_2 - zA)^{-1}\widehat{\boldsymbol{\xi}}}{b^T(I_2 - zA)^{-1}\mathbb{1}} = 1/4,$$

and the condition (B) is satisfied.

The IMEX scheme

$$\begin{array}{c|ccc|ccc} 0 & 0 & 0 & 0 & 0 & 0 & 0 \\ \gamma & 0 & \gamma & 0 & \gamma & 0 & 0 \\ 1-\gamma & 0 & 1-2\gamma & \gamma & 1-\gamma & \gamma-1 & 2(1-\gamma) & 0 \\ \hline & 0 & 1/2 & 1/2 & 0 & 1/2 & 1/2 \end{array}, \quad \gamma = \frac{3+\sqrt{3}}{6}, \quad (3.5)$$

also satisfies the conditions. This pair, which was proposed by Ascher, Ruuth and Spiteri [1], determines a method of order 3 for ODEs. In particular, (2.2) and (2.3) are satisfied. The conditions (A) and (B) follow from

$$\begin{aligned} r(z) &= \frac{1 - (2\gamma - 1)z - (\gamma - 1/3)z^2}{(1 - \gamma z)^2}, \\ (I_3 - zA)^{-1} &= \begin{bmatrix} 1 & 0 & 0 \\ 0 & \frac{1}{1 - \gamma z} & 0 \\ 0 & -\frac{(2\gamma - 1)z}{(1 - \gamma z)^2} & \frac{1}{1 - \gamma z} \end{bmatrix}, \\ zb^T(I_3 - zA)^{-1} &= \frac{z}{2} \left[ 0, \frac{1 - (3\gamma - 1)z}{(1 - \gamma z)^2}, \frac{1}{1 - \gamma z} \right], \\ \phi(z) &= \left( \frac{\gamma^2}{2} \right) \frac{(2\gamma - 1)z}{2 + (1 - 4\gamma)z}, \quad \hat{\phi}(z) = -\frac{\gamma^2(2\gamma - 1)z}{2 + (1 - 4\gamma)z}. \end{aligned}$$

We refer to the scheme (3.5) as the ARS3 scheme.

We apply these schemes to the MOL approximation (3.2), and integrate it from  $t = 0$  to  $t = 1$ , with various grid and step sizes of the form  $h = \Delta t = 1/M$ . We measure the errors for each scheme by

$$\epsilon_M = \max_{1 \leq n \leq M} \| u_n - \mathbf{u}_h(t_n) \|, \quad (3.6)$$

where  $\| \cdot \|$  denotes the discrete  $L_2$  norm, i.e., the induced norm from the inner product

$$\langle u, v \rangle = h \sum_{j=1}^{M-1} u_j v_j, \quad u, v \in \mathbb{R}^{M-1}.$$

The results are summarized in Table 1. The second, fourth and sixth columns give the values of  $\epsilon_M$  for each scheme. The third, fifth and seventh columns

display the order of accuracy for each scheme computed by  $\log_2(\epsilon_{M/2}/\epsilon_M)$ . Order 1 and order 2 are observed for the IMEX Euler scheme (1.7) and the IMEX trapezoidal scheme (3.4), respectively. The observed order for the ARS3 scheme (3.5) is about 2.2.

Table 1

Accuracy test with the model problem (3.1) for the IMEX Runge-Kutta schemes.

| $M$ | IMEX Euler          |       | IMEX TR.            |       | ARS3                |       |
|-----|---------------------|-------|---------------------|-------|---------------------|-------|
|     | $L_2$ -error        | order | $L_2$ -error        | order | $L_2$ -error        | order |
| 10  | $1.4 \cdot 10^{-2}$ |       | $5.7 \cdot 10^{-3}$ |       | $2.6 \cdot 10^{-3}$ |       |
| 20  | $7.5 \cdot 10^{-3}$ | 0.90  | $1.4 \cdot 10^{-3}$ | 1.99  | $5.0 \cdot 10^{-4}$ | 2.37  |
| 40  | $3.9 \cdot 10^{-3}$ | 0.95  | $3.6 \cdot 10^{-4}$ | 2.00  | $1.0 \cdot 10^{-4}$ | 2.31  |
| 80  | $2.0 \cdot 10^{-3}$ | 0.98  | $9.0 \cdot 10^{-5}$ | 2.00  | $2.1 \cdot 10^{-5}$ | 2.24  |
| 160 | $9.9 \cdot 10^{-4}$ | 0.99  | $2.2 \cdot 10^{-5}$ | 2.00  | $4.7 \cdot 10^{-6}$ | 2.20  |
| 320 | $5.0 \cdot 10^{-4}$ | 0.99  | $5.6 \cdot 10^{-6}$ | 2.00  | $1.0 \cdot 10^{-6}$ | 2.22  |
| 640 | $2.5 \cdot 10^{-4}$ | 1.00  | $1.4 \cdot 10^{-6}$ | 2.00  | $2.1 \cdot 10^{-7}$ | 2.23  |

To examine stability of the schemes, we consider the reaction-diffusion equation

$$\frac{\partial \mathbf{u}}{\partial t} = \frac{\partial^2 \mathbf{u}}{\partial x^2} + g(\mathbf{u}), \quad t \geq 0, \quad x \in \Omega, \quad (3.7)$$

with  $g(\mathbf{u}) = \mu \mathbf{u}(1 - \mathbf{u}^2)$ , under the homogeneous Dirichlet condition  $\mathbf{u}(t, 0) = \mathbf{u}(t, 1) = 0$ ,  $t \geq 0$ , where  $\mu$  is a real parameter. Since the eigenvalues of the operator  $d^2/dx^2$  in  $L^2(\Omega)$  with the homogeneous Dirichlet condition are

$$-k^2 \pi^2, \quad k = 1, 2, \dots,$$

if  $\mu < \pi^2$ , the trivial solution  $\mathbf{u} \equiv 0$  is asymptotically stable (see, e.g., [12], Sect. 5.2, Theorem 2.2). In the case  $\mathbf{u}$  represents the concentration of a substance, this means that diffusion suppresses the growth of the substance if the growth rate is relatively small. It seems as if this is easily mimicked using an IMEX scheme.

We again adopt an MOL approximation

$$\frac{du}{dt} = L_h u + g_h(u), \quad (3.8)$$

for the uniform grid  $\Omega_h$  with  $h = 1/M$ , where  $u$  and  $L_h$  are the same as before. The eigenvalues of the matrix  $L_h$  are

$$\lambda_k = -\frac{4}{\Delta x^2} \sin^2\left(\frac{k\pi\Delta x}{2}\right), \quad k = 1, \dots, M-1.$$

If  $\mu < -\lambda_1$ , the trivial solution of (3.8) is asymptotically stable. Fig.1 displays a typical solution in the case  $\mu < -\lambda_1$ . The parameter values are

$$\mu = 8, \quad M = 100, \tag{3.9}$$

and  $\mathbf{u}_0(x) = x(1-x)$ . The asymptotic property is completely preserved by the IMEX Euler scheme (1.7); stable numerical solutions are obtained even for rather large  $\Delta t$ , e.g.,  $\Delta t = 1000$ .

On the other hand, an instability phenomenon is observed for the IMEX trapezoidal scheme (3.4) with rather small  $\Delta t$ . Fig. 2 displays a numerical solution by the IMEX trapezoidal scheme with  $\Delta t = 1/250$ . The solution tends to zero for a while, but irregular oscillation occurs near the ends, which spreads over the whole interval  $\Omega = (0,1)$ . If  $\Delta t$  is sufficiently small, the scheme generates a stable solution. In order to find a value of  $\Delta t$  at which the asymptotic property changes, we take  $\Delta t = 1/k$  for positive integer  $k$ , and plot  $\|u_{100k}\|$  against  $k$  (Fig. 3), where  $u_{100k}$  is an approximate value of  $\mathbf{u}_h(100)$  obtained with  $\Delta t = 1/k$ . Fig. 3 shows that the change occurs near  $\Delta t = 1/280$ . Fig. 4 shows the same results for the ARS3 scheme (3.5). It is observed that the scheme generates a stable solution for larger  $\Delta t$  and the change of the asymptotic behavior occurs near  $\Delta t = 1/20$ .

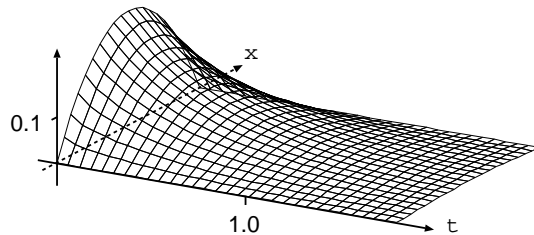


Fig. 1. Exact solution to (3.8) for  $\mu = 8$ ,  $M = 100$ .

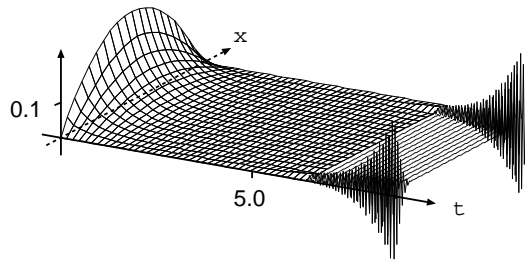


Fig. 2. Numerical solution to (3.8) by the IMEX trapezoidal scheme (3.4).

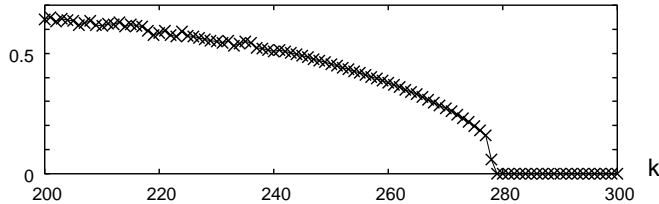


Fig. 3.  $L_2$ -errors at  $t = 100$  versus the partition number  $k$  with  $\Delta t = 1/k$  for the IMEX trapezoidal scheme (3.4).

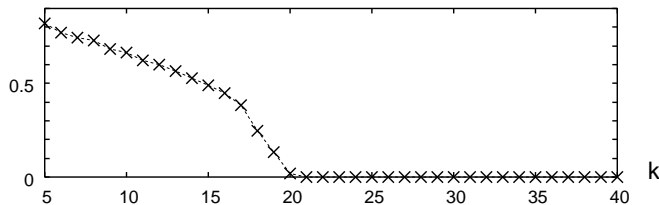


Fig. 4.  $L_2$ -errors at  $t = 100$  versus the partition number  $k$  with  $\Delta t = 1/k$  for the ARS3 scheme (3.5).

#### 4 Stability Analysis of IMEX Runge-Kutta schemes

The asymptotic behavior of numerical solutions to the equation (3.8) is studied on the basis of the scalar test equation

$$\frac{dv}{dt} = \lambda v(t) + \mu v(t), \quad (4.1)$$

which was proposed by Frank, Hundsdorfer and Verwer [4] (see also [13,16]). In fact, using matrix diagonalization, the linearized equation of (3.8) around the trivial solution is converted into a system consisting of equations of this form with  $\lambda = \lambda_k$ ,  $k = 1, \dots, M$ . Under this correspondence, application of the IMEX scheme (1.6) to the test equation (4.1) yields

$$\begin{aligned} V_n &= v_n \mathbb{1} + \Delta t \lambda A V_n + \Delta t \mu \hat{A} V_n, \\ v_{n+1} &= v_n + \Delta t \lambda b^T V_n + \Delta t \mu \hat{b}^T V_n, \end{aligned}$$

where  $V_n \in \mathbb{C}^s$  is an intermediate variable. By Cramer's rule, this implies

$$v_{n+1} = R(\alpha, z)v_n, \quad \alpha = \Delta t\lambda, \quad z = \Delta t\mu,$$

where  $R(\alpha, z)$  is a function defined by

$$R(\alpha, z) = \frac{\det(I - \alpha A - z\hat{A} + \alpha b^T \mathbb{1} + z\hat{b}^T \mathbb{1})}{\det(I - \alpha A)}. \quad (4.2)$$

The function  $R(\alpha, z)$  is an analogue of the stability function of the usual Runge-Kutta method, and it would be reasonable to define the stability region of the IMEX method as

$$S = \{(\alpha, z) \in \mathbb{C}^2 : |R(\alpha, z)| < 1\}. \quad (4.3)$$

It is not easy to comprehend geometric structure of this region. But, in the case of the equation (3.8), the eigenvalues  $\lambda_k$  and the parameter  $\mu$  are both real. The asymptotic behavior of numerical solutions to (3.8) is characterized by the restricted region

$$S^{\text{real}} = S \cap \mathbb{R}^2, \quad (4.4)$$

which is easily visualized, for its boundary is represented with the algebraic curves  $P(\alpha, z) - Q(\alpha) = 0$  and  $P(\alpha, z) + Q(\alpha) = 0$ , where

$$P(\alpha, z) = \det(I - \alpha A - z\hat{A} + \alpha b^T \mathbb{1} + z\hat{b}^T \mathbb{1}), \quad Q(\alpha) = \det(I - \alpha A).$$

For the IMEX Euler scheme (1.7), we have  $R(\alpha, z) = (1+z)/(1-\alpha)$ , and  $S^{\text{real}}$  is given by  $|1+z| < |1-\alpha|$  (Fig. 5). If  $\lambda < 0$  and  $|\mu| < -\lambda$ , then  $(\alpha, z) = (\Delta t\lambda, \Delta t\mu)$  is included in  $S^{\text{real}}$  for any  $\Delta t > 0$ . This confirms the observation that the IMEX Euler scheme generates a stable solution to (3.8) even for very large  $\Delta t$ .

On the other hand, we have

$$R(\alpha, z) = \frac{1 + \alpha/2 + (1 + \alpha/2)z + z^2/2}{1 - \alpha/2},$$

$$S^{\text{real}} : \begin{cases} -2 < z < -\alpha, 2 + (1 + \alpha/2)z + z^2/2 > 0 \text{ for } \alpha < 2, \\ (z > -2 \text{ or } z < -\alpha), 2 + (1 + \alpha/2)z + z^2/2 < 0 \text{ for } \alpha > 2, \end{cases}$$

for the IMEX trapezoidal scheme (3.4). When  $\lambda < 0$  and  $0 < \mu < -\lambda$ , the intersection point of the ray  $(\alpha, z) = (\Delta t \lambda, \Delta t \mu)$ ,  $\Delta t > 0$ , and the quadratic curve  $2 + (1 + \alpha/2)z + z^2/2 = 0$  is given by

$$\Delta t_0 = \frac{4}{\sqrt{(-4\lambda - 3\mu)\mu} - \mu}. \quad (4.5)$$

Hence,  $(\alpha, z) = (\Delta t \lambda, \Delta t \mu)$  is included in  $S^{\text{real}}$  if and only if  $\Delta t < \Delta t_0$ . For a fixed  $\mu > 0$ ,  $\Delta t$  is an increasing function of  $\lambda (< -\mu)$ . When  $M = 100$ , the largest negative eigenvalue of the matrix  $L_h$  of (3.3) is  $\lambda_{99} = -4 \cdot 100^2 \sin^2(99\pi/2/100) \approx -39990.1$ . Thus,  $\Delta t_0 \approx 1/280.8$ , which is obtained by inserting  $\lambda = \lambda_{99}$  and  $\mu = 8$  into (4.5), gives a limit for stability. This confirms the numerical observation of the previous section (Fig. 3).

For the ARS3 scheme (3.5), we have

$$R(\alpha, z) = \frac{6 + 6z + 3z^2 + z^3 - \sqrt{3}\alpha(2 + 2z + z^2) - (1 + \sqrt{3})\alpha^2(1 + z)}{6(1 - \gamma\alpha)^2}.$$

The region  $S^{\text{real}}$  is represented in Fig. 7. The curved boundary in the second quadrant is (a part of) the cubic curve

$$12 + (4\sqrt{3} - 6)\alpha + \alpha^2 + [6 - 2\sqrt{3}\alpha - (1 + \sqrt{3})\alpha^2]z + (3 - \sqrt{3}\alpha)z^2 + z^3 = 0.$$

The intersection point of this curve and the ray  $(\alpha, z) = (\Delta t \lambda_{99}, 8\Delta t)$ ,  $\Delta t > 0$ , is given by  $\Delta t_0 \approx 1/21.7$ , which is computed, e.g., by the Newton-Raphson method. This again coincides with the observed limit for stability (Fig. 4).

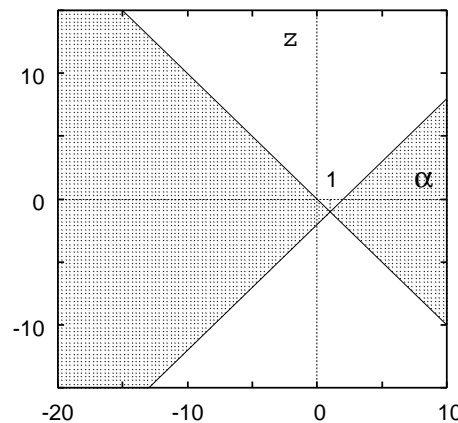


Fig. 5.  $S^{\text{real}}$  of the IMEX Euler scheme (1.7).



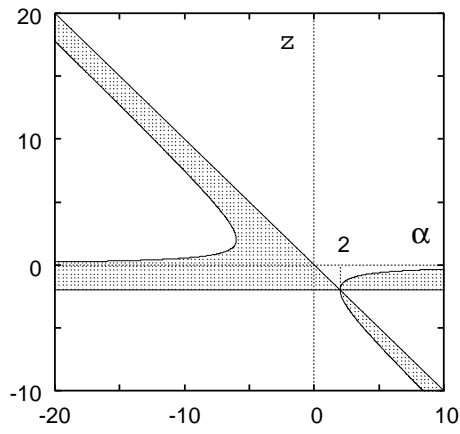


Fig. 6.  $S^{\text{real}}$  of the IMEX trapezoidal scheme (3.4).

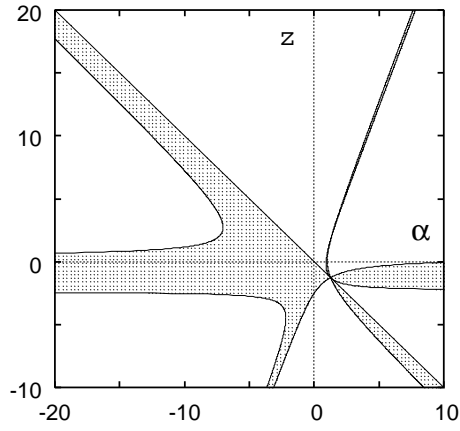


Fig. 7.  $S^{\text{real}}$  of the ARS3 scheme (3.5).

There are IMEX schemes which satisfy all the conditions of Theorem 2.1 and have larger stability regions. The scheme

$$\begin{array}{c|ccc} 0 & 0 & 0 & 0 \\ \omega & 0 & \omega & 0 \\ 1 & 0 & 1 - \omega & \omega \\ \hline & 0 & 1 - \omega & \omega \end{array}, \quad
 \begin{array}{c|ccc} 0 & 0 & 0 & 0 \\ \omega & \omega & 0 & 0 \\ 1 & \kappa & 1 - \kappa & 0 \\ \hline & \kappa & 1 - \kappa & 0 \end{array}, \quad
 \omega = \frac{2 - \sqrt{2}}{2}, \quad \kappa = 1 - \frac{1}{2\omega}. \quad (4.6)$$

was proposed by Ascher, Ruuth and Spiteri [1]. This is constructed on the basis of an  $L$ -stable diagonally implicit method. The scheme

$$\begin{array}{c|cccc} 0 & 0 & 0 & 0 & 0 \\ 1 & 0 & 1 & 0 & 0 \\ \frac{1}{2} & 0 & -\frac{1}{2} & 1 & 0 \\ \hline 1 & 0 & -1 & 1 & 1 \\ \hline 0 & -1 & 1 & 1 & 1 \end{array}, \quad \begin{array}{c|cccc} 0 & 0 & 0 & 0 & 0 \\ 1 & 1 & 0 & 0 & 0 \\ \frac{1}{2} & \frac{1}{2} & 0 & 0 & 0 \\ \hline 1 & 0 & 0 & 1 & 0 \\ \hline 0 & 0 & 1 & 0 & 0 \end{array}. \quad (4.7)$$

was recently proposed by Koto [10]. In [10] we have shown that the left formula gives an  $L$ -stable method and that the scheme (4.7) has an excellent stability property for delay differential equations (DDEs). Both schemes are of order 2 for ODEs.

We have

$$R(\alpha, z) = \frac{1 - \alpha + \sqrt{2}\alpha + (1 - \alpha + \sqrt{2}\alpha)z + z^2/2}{(1 - \omega\alpha)^2}$$

for the scheme (4.6), and

$$R(\alpha, z) = \frac{1 - 2\alpha + \alpha^2/2 + (1 - 2\alpha)z + (1/2 - \alpha)z^2}{(1 - \alpha)^3} \quad (4.8)$$

for the scheme (4.7). The stability regions of these schemes are represented in Fig. 8 and Fig. 9. The linear boundaries of  $S^{\text{real}}$  of the scheme (4.6) are  $z = -\alpha$  and  $z = (3 - 2\sqrt{2})\alpha - 2$ . The region  $S^{\text{real}}$  of the scheme (4.7) coincides with that of the IMEX Euler scheme, except for the range  $1/2 \leq \alpha \leq 3/2$  (the right diagram of Fig. 9). This suggests that the scheme (4.7), constructed for solving DDEs, has a good stability property for reaction-diffusion equations. Further numerical experiments would be expected for examining whether the scheme is really useful for practical reaction-diffusion problems.

**Acknowledgment.** I would like to thank Professor Taketomo Mitsui for his stimulating discussion on numerical methods for differential equations over the past twenty years.

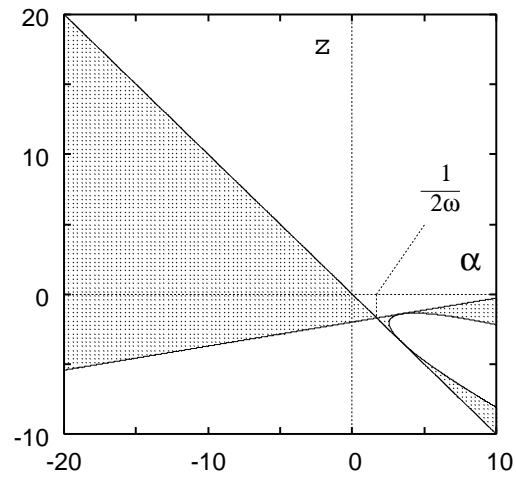


Fig. 8.  $S^{\text{real}}$  of the scheme (4.6).

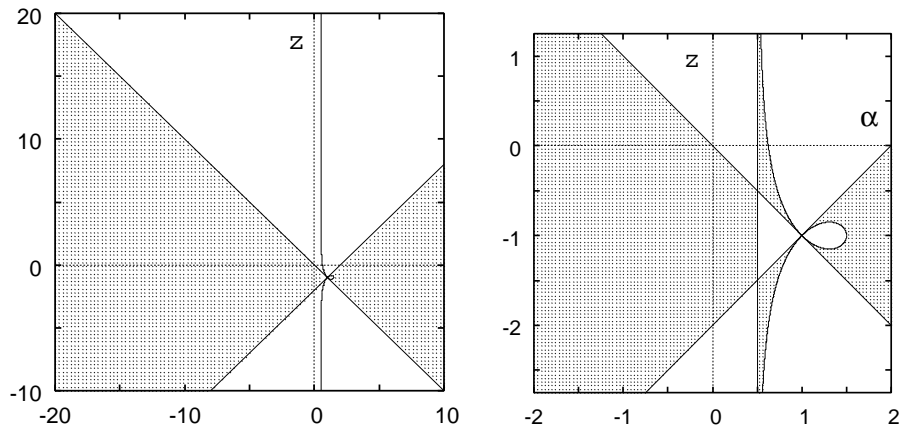


Fig. 9.  $S^{\text{real}}$  of the scheme (4.7)

## References

- [1] U. M. Ascher, S. J. Ruuth, R. J. Spiteri, Implicit-explicit Runge-Kutta methods for time-dependent partial differential equations, *Appl. Numer. Math.* 25 (1997), 151–167.
- [2] K. Burrage, W. H. Hundsdorfer, J. G. Verwer, A study of B-convergence of Runge-Kutta methods, *Computing*, 36 (1986), 17–34.
- [3] M. P. Calvo, J. de Frutos, J. Novo, Linearly implicit Runge-Kutta methods for advection-reaction-diffusion equations, *Appl. Numer. Math.* 37 (2001), 535–549.
- [4] J. Frank, W. Hundsdorfer, J. G. Verwer, On the stability of implicit-explicit linear multistep methods, *Appl. Numer. Math.* 25 (1997), 193–205.
- [5] E. Hairer, G. Wanner, *Solving Ordinary Differential Equations II, Stiff and Differential-Algebraic Problems*, second revised ed., Springer-Verlag, Berlin, 1996.

- [6] D. Hoff, Stability and convergence of finite difference methods for systems of nonlinear reaction-diffusion equations, *SIAM J. Numer. Anal.* **15** (1978), 1161–1177.
- [7] W. Hundsdorfer and J. Verwer, *Numerical Solution of Time-Dependent Advection-Diffusion-Reaction Equations*, Springer-Verlag, Berlin, 2003.
- [8] C. A. Kennedy and M. H. Carpenter, Additive Runge-Kutta schemes for convection-diffusion-reaction equations, *Appl. Numer. Math.* **44** (2003), 139–181.
- [9] T. Koto, Explicit Runge-Kutta schemes for evolutionary problems in partial differential equations, *Ann. Numer. Math.* **1** (1994), 335–346.
- [10] T. Koto, Stability of IMEX Runge-Kutta methods for delay differential equations, *J. Comput. Appl. Math.* (2006), doi: 10.1016/j.cam.2006.11.011.
- [11] J. D. Murray, *Mathematical Biology II, Spatial Models and Biomedical Applications*, third ed., Springer-Verlag, New York, 2003.
- [12] C. V. Pao, *Nonlinear Parabolic and Elliptic Equations*, Plenum Press, New York, 1992.
- [13] L. Pareschi and G. Russo, *Implicit-explicit Runge-Kutta schemes for stiff systems of differential equations*, in: D. Trigiante (Ed.), *Recent Trends in Numerical Analysis*, Nova Science Publishers Inc., Huntington, NY, 2001, pp. 269–288.
- [14] J. M. Sanz-Serna, J. G. Verwer, W. H. Hundsdorfer, Convergence and order reduction of Runge-Kutta schemes applied to evolutionary problems in partial differential equations, *Numer. Math.* **50** (1986), 405–418.
- [15] J. G. Verwer, Convergence and order reduction of diagonally implicit Runge-Kutta schemes in the method of lines, in: D. F. Griffiths, G. A. Watson (Ed.), *Numerical Analysis (Dundee, 1985)*, Pitman Res. Notes Math. Ser. 140, Longman Scientific & Technical, Harlow, 1986, pp. 220–237.
- [16] J. G. Verwer, B. P. Sommeijer, An implicit-explicit Runge-Kutta-Chebyshev scheme for diffusion-reaction equations, *SIAM J. Sci. Comput.* **25** (2004), 1824–1835.